Contribution from the Department of Chemistry, University of Colorado, Boulder, Colorado 80309, and the School of Chemical Sciences, University of Illinois, Urbana, Illinois 61801

Magnetic Exchange Interactions in Transition Metal Dimers. 11. Structural and Magnetic Characterization of Two Chloranilate-Bridged Dimeric Complexes $[Ni_2(tren)_2(C_6O_4Cl_2)](BPh_4)_2$ and $[Cu_2(Me_5dien)_2(C_6O_4Cl_2)](BPh_4)_2$. Magnetic Exchange Interactions Propagated by the Dianions of 2,5-Dihydroxy-1,4-benzoquinones[1]

CORTLANDT G. PIERPONT,*[2] LYNN C. FRANCESCONI,[3] and DAVID N. HENDRICKSON*[3,4]

Received February 25, 1977 AIC70152S

The structures of $[Ni_2(tren)_2(CA)](BPh_4)_2$ and $[Cu_2(Me_5dien)_2(CA)](BPh_4)_2$, where CA^{2-} is the dianion of chloranilic acid ($O_4C_6H_2Cl_2$), tren is 2,2′,2″-triaminotriethylamine, and Me_5dien is 1,1,4,7,7-pentamethyldiethylenetriamine, have been determined using heavy-atom, x-ray methods. The nickel compound crystallizes in the monoclinic space group $P2_1/c$ with two formula weights in a unit cell of dimensions $a = 9.883$ (2) Å, $b = 16.326$ (4) Å, $c = 21.763$ (4) Å, $\beta = 118.93$ (2)°, d(calcd) = 1.355 g cm^{-3}, and d(exptl) = 1.352 (4) g cm^{-3}. The structure was refined to conventional discrepancy factors of $R = 0.059$ and $R_w = 0.063$ for 3659 observed reflections. The copper compound crystallizes in the monoclinic space group $P2_1/a$ with two formula weights in a unit cell of dimensions $a = 23.432$ (5) Å, $b = 9.933$ (2) Å, $c = 15.039$ (3) Å, $\beta = 98.00$ (2)°, d(calcd) = 1.256 g cm^{-3}, and d(exptl) = 1.253 (5) g cm^{-3}. The copper compound was refined to give $R = 0.061$ and $R_w = 0.068$ for 2951 observed reflections. Both of these compounds are BPh_4^- salts of centrosymmetric metal complexes which are bridged in a bis-bidentate fashion by the dianion of chloranilic acid. The nickel ion coordination geometry is pseudooctahedral in $[Ni_2(tren)_2(CA)]^{2+}$, whereas the copper ion coordination in $[Cu_2(Me_5dien)_2(CA)]^{2+}$ is five-coordinate and intermediate between trigonal bipyramidal and square pyramidal. In these two dimers the chloranilate dianion coordinates unsymmetrically at each metal ion with the greater asymmetry in the copper compound where at each metal Cu–O lengths of 1.956 (4) and 2.196 (4) Å were found. The chloranilate dianion is planar in each dimer and has a localized quinonoid structure with four short C–C bond lengths and two long (single) bond lengths (e.g., 1.381 (6) and 1.536 (6) Å, respectively). Variable-temperature (4.2–270 K) magnetic susceptibility and EPR data are reported for the two structurally characterized compounds as well as two other analogous Ni(II) and three analogous Cu(II) complexes. Antiferromagnetic exchange interactions are seen for the three nickel compounds; the exchange parameter for the CA^{2-} compound is $J = -1.8$ cm^{-1} in spite of the fact that the Ni–Ni distance in the dimer is 7.937 (2) Å. The exchange interaction in the four copper dimers is found to be very sensitive to the nonbridging ligand. No indications of an exchange interaction are found in the susceptibility data to 4.2 K for the two Me_5dien copper 2,5-dihydroxy-1,4-benzoquinone dianion-bridged dimers. The observation of singlet-to-triplet EPR transitions for these two dimers sets their exchange parameters at $|J| = 0.1$ cm^{-1}. The compound $[Cu_2(dpt)_2(CA)](BPh_4)_2$, where dpt is dipropylenetriamine, and an analogous compound have exchange parameters ($J = -2.0$ and -4.6 cm^{-1}, respectively) that are very close to the parameter ($J = -5.7$ cm^{-1}) for the oxalate-bridged $[Cu_2(dpt)_2(Ox)](BPh_4)_2$. The exchange interactions in these compounds are compared with previously reported interactions, and a molecular orbital analysis is presented to qualitatively explain the observed variations.

Introduction

Benzoquinones are well known as versatile redox reagents and are among the most pervasive natural products on the earth's surface. They are present in most living organisms and are found in the ubiquitous humic substances.[5] The coordination chemistry of quinones with transition metals has not been well developed. Three basic types of quinone interactions with metals and metal complexes have been noted. Donor–acceptor complexes where there is no direct interaction between quinone and metal have been investigated. These form by pairing of quinone and ligand π orbitals as in the bis(8-hydroxyquinolinato)palladium(II) chloranil complex.[6] *p*-Quinones, most notably duroquinone, bond with nucleophilic metals as localized diene ligands. Bis(duroquinone)nickel(0) is a particular example of this coordination.[7] *o*-Quinones, however, form chelated complexes as oxygen-donor ligands. A vacant and readily accessible quinone π^* level enables π-acceptor activity with appropriate metals. Accordingly, *o*-quinone complexes have been characterized with reduced (catecholate), oxidized, and partially reduced (semiquinone) ligands.[8]

Only a few dimeric transition metal complexes have been reported with quinones or quinone derivatives as bridging units. The Mo(VI) complex of composition $Mo_2(O_2C_6Cl_4)_6$ has been characterized from the reaction of tetrachloro-1,2-benzoquinone with $Mo(CO)_6$.[9] The two molybdenum ions are each chelated by two reduced quinone ligands with two reduced ligands bridging the metal centers. Pentacyanocobaltate anion and *p*-benzoquinone give[10] the species $[(CN)_5Co(OC_6H_4O)Co(CN)_5]^{6-}$. Apparently dimeric complexes with the formula of $[M(salen)]_2$(*p*-quinone), M = Fe and Co and salen = *N*,*N*-ethylenebis(salicylideniminato), have been reported.[11]

In this paper, we report the synthesis and characterization of several dimeric Ni(II) and Cu(II) complexes bridged by the dianions of two 2,5-dihydroxy-1,4-benzoquinones (I) and

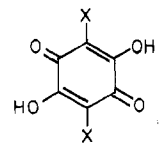

Ia, X = H
b, X = Cl (chloranilic acid)

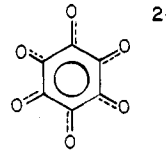

II

the rhodizonate dianion (II). *Polymeric* first-row transition metal complexes have been prepared with the dianions of both of the above 2,5-dihydroxy-1,4-benzoquinones.[12,13] Magnetic susceptibility measurements between 1.4 and 80 K have shown that the two polymeric Cu(II) compounds exhibit antiferromagnetism characteristic of a linear chain.[14] Sartene and Boutron[15] have presented a theoretical analysis of the exchange parameter associated with a magnetic exchange interaction between two Cu(II) ions as propagated by the dianion of 2,5-dihydroxy-1,4-benzoquinone. Because of the uncertainties of determining an exchange parameter for a polymeric compound, particularly one of unknown structure, it was of interest to determine the magnetic exchange present in a structurally characterized Cu(II) dimer with such a bridge. It was also our intent to compare the viability of the di-

hydroxy–benzoquinone dianion bridge for propagating exchange interactions with those of the oxalate and squarate dianions as characterized in previous papers.[1,16-18] Finally, it was also a goal of the present work to ascertain the molecular dimensions of one of the above dihydroxyquinone dianions as it is coordinated to a transition metal ion and to compare the dimensions with structural data for Ib[19] and data for the potassium salt[20] of Ia and the ammonium salt[21] of Ib.

Experimental Section

Compound Preparation. Reagent grade materials were used as purchased. Analyses were performed in the University of Illinois School of Chemical Sciences microanalytical laboratory; all analytical data are collected in Table I.[22]

All seven compounds were prepared in a similar fashion and it will suffice to detail the typical preparation of $[Ni_2(tren)_2(CA)](BPh_4)_2$, where CA^{2-} is the dianion of chloranilic acid Ib, and tren is 2,2′,2″-triaminotriethylamine. Approximately 0.5 g (2 mmol) of $NiSO_4 \cdot 6H_2O$ is dissolved in ~150 mL of H_2O and, then, ~0.4 mL (3.8 mmol) of tren is added. A ~150-mL H_2O solution containing ~0.2 g (1 mmol) of chloranilic acid is added to the first solution. The resulting solution is filtered through a medium-porosity frit and with vigorous stirring a filtered aqueous solution of $NaBPh_4$ is added to give a brown precipitate. The solid is vacuum filtered and washed several times with H_2O followed by several washings with diethyl ether. The solid is then dried overnight in vacuo over P_4O_{10}. When so dried, these tetraphenylborate salts are relatively electrostatic.

The copper compounds were generally prepared with $Cu(ClO_4)_2 \cdot 6H_2O$. Crystals of $[Ni_2(tren)_2(CA)](BPh_4)_2$ and $[Cu_2(Me_5dien)_2(CA)](BPh_4)_2$, where Me_5dien is 1,1,4,7,7-pentamethyldiethylenetriamine, were obtained by slow evaporation of CH_3CN solutions. The two Me_5dien copper compounds were recrystallized from three solvents (acetonitrile, acetone, and nitromethane) to give different crystalline samples to check the reproducibility of weak EPR signals (vide infra).

Physical Measurements. Magnetic susceptibilities (4.2–270 K) were determined with a PAR Model 150A vibrating-sample magnetometer at a field setting of 12.7 kG. A sample of $CuSO_4 \cdot 5H_2O$ was used as a standard, and all data were corrected for background, sample diamagnetism,[23] and sample TIP (taken as 120×10^{-6} cgsu per copper dimer or as 200×10^{-6} cgsu per nickel dimer). Two complete magnetic susceptibility data sets were collected for samples of $[Ni_2(tren)_2(CA)](BPh_4)_2$ and $[Ni_2(tren)_2(DHBQ)]BPh_4)_2$ and the data were found to be reproducible within experimental error. A computer program incorporating the minimization subprogram STEPT[24] was used to least-squares fit the susceptibility data to theoretical equations.

EPR spectra were recorded on Varian E-9 X-band and E-15 Q-band spectrometers. Low temperatures were obtained on the X-band unit with an Air Products Heli-tran liquid-helium cooling system and a carbon resistor sensing element.

Structure Determination of $[Ni_2(tren)_2(O_4C_6Cl_2)](BPh_4)_2$. A crystal of the nickel chloranilate complex was mounted and centered on a Syntex $P\bar{1}$ computer-controlled diffractometer equipped with a graphite-crystal monochromator. Photographs taken on other crystals indicated monoclinic symmetry with extinction patterns consistent with space group $P2_1/c$. The centered settings of 15 reflections were refined by least-squares procedures and used to calculate the cell constants given in Table II. Data were collected by the θ–2θ scan technique at a scan rate of 2.0°/min. Four standard reflections, measured after every 100 reflections, showed only normal variations in intensity. The data set was collected up to a 2θ (Mo Kα) value of 50° using a symmetrical scan range of ±0.6°. Corrections were applied for Lorentz and polarization effects. Due to the small variation in transmission coefficients, no correction for absorption was applied. Of the 6279 reflections measured, 3659 were found to have $F_o^2 > 3\sigma(F_o^2)$ and were used in the refinement.[25]

The nickel atom position was determined from a three-dimensional Patterson map. Least-squares refinement of its positional and isotropic thermal parameters gave discrepancy factors

$$R = (\Sigma ||F_o| - |F_c||)/\Sigma |F_o| = 0.551$$

$$R_w = [\Sigma w(|F_o| - |F_c|)^2/wF_o^2]^{1/2} = 0.603$$

where w is the weighting factor set as $4F_o^2/\sigma^2(F_o^2)$ and $|F_o|$ and $|F_c|$ are the observed and calculated structure factors, respectively. The atomic scattering factors used for the nonhydrogen atoms were those of Cromer and Waber,[26] and hydrogen scattering factors were obtained from Stewart et al.[27] Anomalous dispersion terms for Ni and Cl were obtained from Cromer and Liberman.[28] A difference Fourier map calculated from the Ni refinement revealed the positions of all nonhydrogen atoms of the structure. The $[Ni_2(tren)_2(O_4C_6Cl_2)]^{2+}$ cations are located about inversion centers at $^1/_2$, 0, 0 and $^1/_2$, $^1/_2$, $^1/_2$, positions 2b of the space group. Two cycles of isotropic refinement of all nonhydrogen atoms gave discrepancy indices of $R = 0.079$ and $R_w = 0.106$. Two additional cycles of anisotropic refinement converged with $R = 0.068$ and $R_w = 0.074$. In all calculations the phenyl rings of the anion were treated as rigid groups with a C–C bond length of 1.392 Å. Corrections were then applied for all hydrogen atoms of the structure assuming a C–H bond length of 0.95 Å and a N–H length of 0.87 Å. Two additional cycles of anisotropic refinement converged with $R = 0.059$ and $R_w = 0.063$. The estimated standard deviation of an observation of unit weight at convergence of the refinement was 1.36. Final positional and thermal parameters of atoms and groups are presented in Tables III and IV. A table of the final values of $|F_o|$ and $|F_c|$ is available.[22]

Table II. Crystal Data for $[Ni_2(tren)_2(O_4C_6Cl_2)](B(C_6H_5)_4)_2$

Formula weight 1254.02	$V = 3073.3$ (11) Å^3
Monoclinic	Mo Kα radiation
Space group $P2_1/c$	$\mu = 7.56$ cm^{-1}
$a = 9.883$ (2) Å	d(exptl) = 1.352 (4) g cm^{-3}
$b = 16.326$ (4) Å	d(calcd) = 1.355 g cm^{-3} for $Z = 2$
$c = 21.763$ (4) Å	Crystal size
$\beta = 118.93$ (2)°	0.45 × 0.32 × 0.29 mm

Structure Determination of $[Cu_2(Me_5dien)_2(O_4C_6Cl_2)](BPh_4)_2$. Precession and Weissenberg photographs taken on crystals of $[Cu_2(Me_5dien)_2(O_4C_6Cl_2)](BPh_4)_2$ indicated monoclinic symmetry with an extinction pattern consistent with space group $P2_1/a$. The centered settings of 15 reflections with 2θ values greater than 20° were refined by least-squares procedures and used to calculate the refined cell constants given in Table V. As before, the dimeric cation is located about a crystallographic inversion center (0, 0, 0; $^1/_2$, $^1/_2$, 0). Data were collected and processed as before.[24] A total of 5321 reflections were measured within the angular range $2.5 \leq 2\theta \leq 45°$. Once again absorption effects were found to be insignificant, so no correction was applied.

The structure was solved using conventional Patterson and Fourier methods. Phenyl rings associated with the independent anion were treated as rigid groups. Refinement was carried out as described in the previous section. All nonhydrogen atoms of the cation and the boron of the anion were refined anisotropically. Group atoms were refined with individual isotropic thermal parameters. In the final cycles fixed contributions for all hydrogen atoms of the structure were included. Final discrepancy indices of $R = 0.061$ and $R_w = 0.068$ were obtained for 2951 observed reflections. The final positional and thermal parameters of the structure are given in Table VI. Derived positional and thermal parameters of group atoms are given in Table VII. A table of the final F_o and $|F_c|$ values may be obtained.[22]

Results and Discussion

In this section the following abbreviations will be used: CA^{2-} for the dianion from chloranilic acid (Ib), $DHBQ^{2-}$ for the dianion from 2,5-dihydroxy-1,4-benzoquinone (Ia), RHZ^{2-} for the dianion II from rhodizonic acid, tren for 2,2′,2″-triaminotriethylamine, Me_5dien for 1,1,4,7,7-pentamethyldiethylenetriamine, dpt for dipropylenetriamine.

Structure of $[Ni_2(tren)_2(CA)](BPh_4)_2$. The nickel chloranilate compound consists of discrete $[Ni_2(tren)_2(CA)]^{2+}$ cations and BPh_4^- anions. The $[Ni_2(tren)_2(CA)]^{2+}$ cation is located about a crystallographic inversion center. A view of the cation is presented in Figure 1 with principal interatomic distances and angles given in Table VIII. The chloranilate ligand bridges two six-coordinate Ni^{2+} ions, chelating to each unsymmetrically. The Ni–Ni distance in the dimer is 7.937 (2) Å. The metal ions are contained within the ligand plane (Table IX). This mode of chloranilate coordination differs considerably from that encountered in the Pd^{2+} complexes $[Pd(CA)Cl_2]^{2-}$ and $[Pd(CA)Cl]_2^{2-}$.[29] In both structures the ligand bonds ostensibly as a dicarbanion, chelating through

Table III. Final Structural Parameters for $[Ni_2(tren)_2(O_4C_6Cl_2)](B(C_6H_5)_4)_2$

Atom[a]	x	y	z	β_{11}[b]	β_{22}	β_{33}	β_{12}	β_{13}	β_{23}
Ni	−0.16707 (7)	0.16339 (4)	0.09992 (3)	0.00833 (9)	0.00196 (2)	0.00234 (2)	−0.00102 (4)	0.00163 (3)	−0.00028 (2)
Cl	−0.24369 (14)	−0.13927 (7)	0.05534 (8)	0.00934 (18)	0.00213 (5)	0.00345 (5)	0.00019 (7)	0.00206 (7)	0.00004 (4)
O(1)	−0.4106 (4)	0.1573 (2)	0.0329 (2)	0.0092 (5)	0.0018 (1)	0.0031 (1)	−0.0009 (2)	0.0013 (2)	−0.0002 (1)
O(2)	−0.2030 (3)	0.0406 (2)	0.0805 (2)	0.0076 (5)	0.0020 (1)	0.0026 (1)	−0.0008 (2)	0.0016 (2)	−0.0003 (1)
C(1)	−0.4622 (5)	0.0853 (3)	0.0153 (2)	0.0088 (7)	0.0020 (2)	0.0018 (1)	−0.0012 (3)	0.0014 (3)	−0.0001 (1)
C(2)	−0.3395 (5)	0.0173 (3)	0.0431 (2)	0.0073 (6)	0.0021 (2)	0.0018 (1)	−0.0005 (3)	0.0017 (3)	−0.0001 (1)
C(3)	−0.3844 (5)	−0.0639 (3)	0.0256 (3)	0.0076 (6)	0.0019 (2)	0.0021 (2)	−0.0002 (3)	0.0018 (3)	−0.0002 (1)
N(1)	−0.1149 (5)	0.2878 (2)	0.1173 (2)	0.0109 (6)	0.0021 (2)	0.0031 (2)	−0.0010 (3)	0.0025 (3)	0.0000 (1)
N(2)	−0.2278 (5)	0.1782 (3)	0.1798 (2)	0.0141 (7)	0.0029 (2)	0.0035 (2)	−0.0007 (3)	0.0041 (3)	−0.0001 (1)
N(3)	0.0658 (4)	0.1492 (2)	0.1675 (2)	0.0090 (6)	0.0025 (2)	0.0031 (2)	0.0000 (2)	0.0020 (2)	−0.0001 (1)
N(4)	−0.1558 (6)	0.1891 (3)	0.0060 (3)	0.0188 (9)	0.0047 (2)	0.0026 (2)	−0.0029 (4)	0.0029 (3)	−0.0002 (2)
C(4)	−0.1969 (7)	0.3193 (3)	0.1548 (3)	0.0157 (10)	0.0023 (2)	0.0051 (3)	−0.0002 (4)	0.0059 (4)	−0.0006 (2)
C(5)	−0.1779 (7)	0.2601 (3)	0.2113 (3)	0.0190 (11)	0.0029 (2)	0.0041 (2)	−0.0023 (4)	0.0065 (4)	−0.0013 (2)
C(6)	0.0554 (6)	0.2983 (3)	0.1606 (3)	0.0111 (8)	0.0023 (2)	0.0035 (2)	−0.0016 (3)	0.0029 (3)	−0.0005 (1)
C(7)	0.1439 (6)	0.2218 (3)	0.1598 (3)	0.0075 (7)	0.0034 (2)	0.0034 (2)	−0.0007 (3)	0.0021 (3)	0.0000 (2)
C(8)	−0.1765 (7)	0.3252 (4)	0.0469 (4)	0.0156 (10)	0.0033 (3)	0.0036 (2)	−0.0004 (4)	0.0023 (4)	0.0014 (2)
C(9)	−0.1237 (8)	0.2773 (4)	0.0030 (3)	0.0193 (12)	0.0055 (3)	0.0025 (2)	−0.0030 (5)	0.0021 (4)	0.0013 (2)
B	−0.4386 (9)	0.0304 (5)	0.3029 (4)	0.0076 (11)	0.0030 (4)	0.0019 (2)	0.0003 (5)	0.0021 (4)	0.0000 (2)

Group[c]	x_c	y_c	z_c	ϕ	θ	ρ
R(1)	−0.1352 (4)	0.0249 (2)	0.2961 (2)	2.433 (5)	2.313 (3)	0.824 (5)
R(2)	−0.3913 (4)	−0.0985 (2)	0.4148 (2)	−0.038 (4)	−2.372 (2)	−1.730 (4)
R(3)	−0.7317 (3)	−0.0105 (2)	0.1626 (2)	2.627 (4)	−2.303 (3)	2.255 (4)
R(4)	−0.5249 (4)	0.2011 (2)	0.3330 (2)	2.147 (3)	−2.492 (3)	−2.681 (4)

[a] Estimated standard deviations of the least significant figures are given in parentheses here and in succeeding tables. [b] Anisotropic thermal parameters are in the form $\exp[-(h^2\beta_{11} + k^2\beta_{22} + l^2\beta_{33} + 2hk\beta_{12} + 2hl\beta_{13} + 2kl\beta_{23})]$. [c] x_c, y_c, and z_c are the fractional coordinates of the rigid group centers. The angles ϕ, θ, and ρ are in radians and have been defined previously: R. Eisenberg and J. A. Ibers, *Inorg. Chem.*, 4, 773 (1965).

Table IV. Derived Positional and Isotropic Thermal Parameters for Group Carbon Atoms in $[Ni_2(tren)_2(O_4C_6Cl_2)](B(C_6H_5)_4)_2$

Atom	x	y	z	B, Å^2
		R(1)		
C(1)	−0.2749 (4)	0.0276 (3)	0.2972 (2)	2.7 (1)
C(2)	−0.1438 (6)	0.0642 (3)	0.3509 (2)	4.6 (2)
C(3)	−0.0042 (5)	0.0615 (4)	0.3499 (3)	5.6 (2)
C(4)	0.0044 (5)	0.0223 (4)	0.2951 (3)	4.8 (2)
C(5)	−0.1266 (6)	−0.0143 (3)	0.2414 (3)	4.4 (2)
C(6)	−0.2663 (5)	−0.0116 (3)	0.2424 (2)	3.1 (1)
		R(2)		
C(1)	−0.4126 (5)	−0.0394 (2)	0.3648 (2)	2.7 (1)
C(2)	−0.4057 (6)	−0.1219 (2)	0.3505 (2)	3.2 (1)
C(3)	−0.3844 (6)	−0.1809 (2)	0.4005 (3)	3.8 (1)
C(4)	−0.3700 (7)	−0.1575 (3)	0.4649 (2)	4.4 (2)
C(5)	−0.3769 (7)	−0.0750 (3)	0.4792 (2)	4.7 (2)
C(6)	−0.3982 (6)	−0.0160 (2)	0.4292 (2)	3.7 (1)
		R(3)		
C(1)	−0.5975 (4)	0.0057 (3)	0.2252 (2)	2.4 (1)
C(2)	−0.6188 (4)	0.0406 (3)	0.1628 (2)	3.5 (1)
C(3)	−0.7530 (5)	0.0243 (3)	0.1001 (2)	3.9 (2)
C(4)	−0.8659 (4)	−0.0268 (3)	0.0999 (2)	3.9 (2)
C(5)	−0.8447 (4)	−0.0616 (3)	0.1624 (2)	3.5 (1)
C(6)	−0.7105 (5)	−0.0454 (3)	0.2250 (2)	2.6 (1)
		R(4)		
C(1)	−0.4826 (5)	0.1246 (2)	0.3197 (2)	2.5 (1)
C(2)	−0.4107 (5)	0.1949 (3)	0.3133 (3)	3.3 (1)
C(3)	−0.4530 (6)	0.2714 (2)	0.3267 (3)	4.0 (2)
C(4)	−0.5672 (6)	0.2776 (2)	0.3464 (3)	4.0 (2)
C(5)	−0.6391 (5)	0.2073 (3)	0.3527 (3)	4.0 (2)
C(6)	−0.5968 (5)	0.1308 (2)	0.3394 (3)	3.0 (1)

Table V. Crystal Data for $[Cu_2(Me_5dien)_2(O_4C_6Cl_2)](BPh_4)_2$

Formula weight 1258.85	V = 3466.4 (10) Å^3
Monoclinic	Mo Kα radiation
Space group $P2_1/a$	μ = 7.70 cm^{-1}
a = 23.432 (5) Å	d(exptl) = 1.253 (5) g cm^{-3}
b = 9.933 (2) Å	d(calcd) = 1.256 g cm^{-3} for Z = 2
c = 15.039 (3) Å	Crystal size
β = 98.00 (2)°	0.41 × 0.38 × 0.28 mm

the 3 and 6 carbon atoms. While the C–O lengths of the palladium structures are slightly longer (1.27–1.29 Å) than

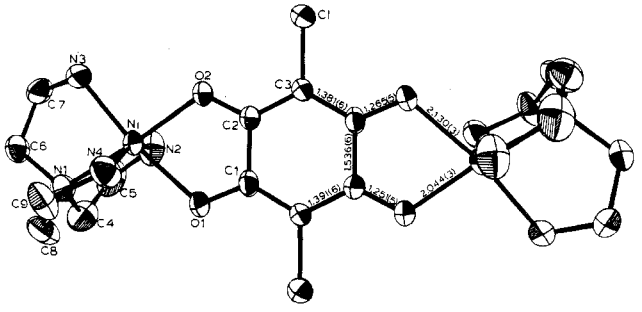

Figure 1. ORTEP plotting of $[Ni_2(tren)_2(CA)]^{2+}$. Hydrogen atoms are not shown.

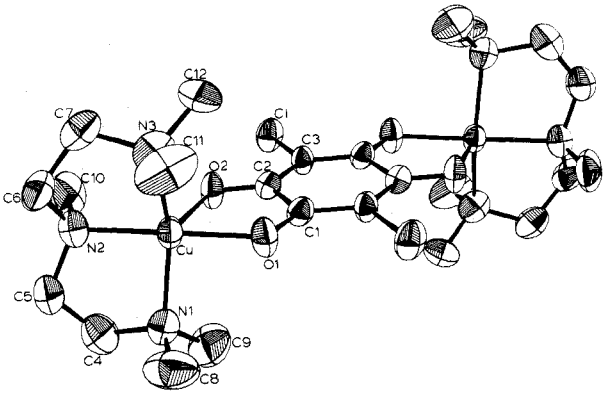

Figure 2. ORTEP plotting of $[Cu_2(Me_5dien)_2(CA)]^{2+}$. Hydrogen atoms are not shown.

those reported for the free chloranilate anion, 1.243 (7) and 1.253 (7) Å,[21] the ring C–C lengths and the presence of

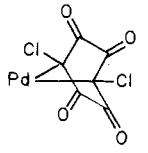

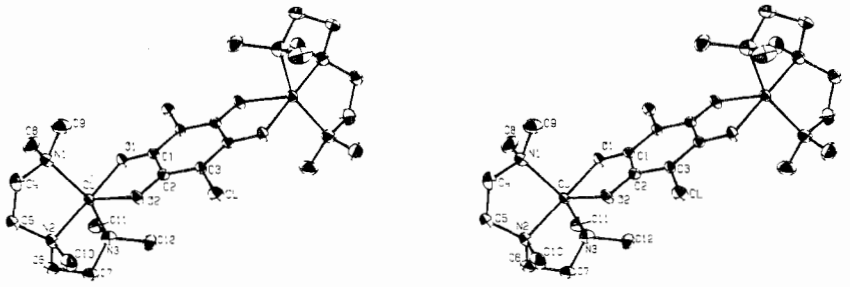

Figure 3. Stereoscopic view of $[Cu_2(Me_5dien)_2(CA)]^{2+}$.

Table VI. Final Structural Parameters for $[Cu_2(Me_5dien)_2(O_4C_6Cl_2)](BPh_4)_2$

Atom	x	y	z	β_{11}	β_{22}	β_{33}	β_{12}	β_{13}	β_{23}
Cu	0.09061 (3)	0.18260 (8)	0.20446 (5)	0.00129 (1)	0.00913 (10)	0.00359 (4)	0.00010 (3)	−0.00022 (2)	−0.00079 (6)
Cl	0.08256 (7)	−0.25393 (18)	0.01389 (12)	0.00169 (4)	0.00939 (21)	0.00604 (11)	0.00147 (8)	−0.00024 (5)	−0.00062 (12)
O(1)	0.0203 (2)	0.2029 (4)	0.1189 (3)	0.0018 (1)	0.0092 (6)	0.0045 (3)	0.0008 (2)	−0.0008 (1)	−0.0019 (3)
O(2)	0.0889 (2)	−0.0096 (4)	0.1320 (3)	0.0015 (1)	0.0102 (6)	0.0046 (3)	0.0010 (2)	−0.0010 (1)	−0.0011 (3)
C(1)	0.0082 (2)	0.1113 (7)	0.0617 (4)	0.0011 (1)	0.0075 (8)	0.0040 (4)	0.0004 (3)	0.0001 (2)	−0.0007 (5)
C(2)	0.0484 (2)	−0.0124 (6)	0.0692 (4)	0.0012 (1)	0.0081 (9)	0.0038 (3)	0.0002 (3)	0.0002 (2)	0.0001 (4)
C(3)	0.0373 (2)	−0.1148 (6)	0.0070 (4)	0.0012 (1)	0.0082 (8)	0.0034 (3)	0.0010 (3)	−0.0003 (2)	−0.0008 (4)
N(1)	0.0464 (2)	0.1509 (7)	0.3101 (4)	0.0017 (1)	0.0171 (10)	0.0050 (3)	−0.0005 (3)	0.0000 (2)	−0.0001 (5)
N(2)	0.1619 (2)	0.1713 (7)	0.2925 (3)	0.0018 (1)	0.0159 (9)	0.0042 (3)	−0.0001 (3)	−0.0004 (1)	0.0001 (4)
N(3)	0.1368 (2)	0.3028 (6)	0.1300 (4)	0.0022 (1)	0.0093 (7)	0.0069 (4)	0.0006 (3)	0.0006 (2)	0.0009 (4)
C(4)	0.0901 (4)	0.1072 (12)	0.3849 (6)	0.0030 (2)	0.0307 (20)	0.0043 (5)	−0.0003 (6)	−0.0001 (3)	0.0015 (8)
C(5)	0.1452 (3)	0.1742 (11)	0.3827 (5)	0.0021 (2)	0.0239 (19)	0.0043 (4)	−0.0012 (5)	−0.0004 (2)	−0.0009 (7)
C(6)	0.1972 (3)	0.2904 (9)	0.2732 (6)	0.0015 (2)	0.0189 (15)	0.0070 (5)	−0.0015 (4)	0.0002 (2)	−0.0030 (7)
C(7)	0.1969 (3)	0.3042 (9)	0.1755 (6)	0.0017 (1)	0.0140 (13)	0.0078 (5)	−0.0010 (4)	0.0007 (2)	−0.0003 (7)
C(8)	0.0171 (4)	0.2760 (9)	0.3285 (7)	0.0040 (3)	0.0174 (13)	0.0091 (7)	−0.0017 (4)	0.0030 (3)	−0.0046 (7)
C(9)	0.0037 (4)	0.0407 (10)	0.2982 (7)	0.0027 (2)	0.0235 (14)	0.0091 (7)	−0.0031 (5)	0.0010 (3)	0.0016 (8)
C(10)	0.1940 (3)	0.0446 (10)	0.2758 (6)	0.0025 (2)	0.0185 (13)	0.0058 (5)	0.0032 (4)	−0.0010 (3)	0.0012 (7)
C(11)	0.1121 (4)	0.4392 (8)	0.1284 (7)	0.0031 (2)	0.0097 (10)	0.0131 (8)	0.0011 (4)	0.0024 (4)	0.0038 (7)
C(12)	0.1355 (4)	0.2574 (10)	0.0358 (5)	0.0029 (2)	0.0217 (13)	0.0045 (4)	−0.0003 (5)	0.0011 (2)	0.0023 (6)
B	0.1394 (3)	0.2792 (8)	−0.2873 (5)	0.0016 (2)	0.0080 (10)	0.0044 (4)	0.0007 (3)	0.0001 (2)	0.0000 (5)

Group	x_c	y_c	z_c	ϕ	θ	ρ
R(1)	0.1977	0.4062	−0.4380	−2.376	3.158	0.896
R(2)	0.0073	0.3146	−0.3095	1.512	2.644	1.573
R(3)	0.1454	−0.0296	−0.2787	−3.100	−2.579	−1.513
R(4)	0.2073	0.4233	−0.1234	−2.377	3.109	−0.769

Table VII. Derived Positional and Isotropic Thermal Parameters for Group Carbon Atoms in $[Cu_2(Me_5dien)_2(O_4C_6Cl_2)](B(C_6H_5)_4)_2$

Atom	x	y	z	B, Å^2
		R(1)		
C(1)	0.1701 (6)	0.3468 (10)	−0.3716 (8)	3.4 (2)
C(2)	0.1479 (5)	0.4639 (12)	−0.4138 (7)	4.1 (3)
C(3)	0.1755 (6)	0.5233 (13)	−0.4802 (8)	5.1 (3)
C(4)	0.2252 (6)	0.4656 (12)	−0.5043 (9)	4.9 (2)
C(5)	0.2474 (5)	0.3484 (11)	−0.4622 (8)	4.6 (3)
C(6)	0.2199 (6)	0.2890 (12)	−0.3958 (7)	3.7 (2)
		R(2)		
C(1)	−0.0213 (5)	0.3182 (11)	−0.2343 (8)	5.5 (3)
C(2)	0.0386 (5)	0.3101 (11)	−0.2239 (8)	4.5 (3)
C(3)	0.0672 (6)	0.3065 (12)	−0.2991 (7)	3.4 (2)
C(4)	0.0359 (5)	0.3109 (13)	−0.3847 (8)	5.1 (2)
C(5)	−0.0239 (6)	0.3190 (12)	−0.3951 (8)	6.1 (2)
C(6)	−0.0525 (6)	0.3226 (12)	−0.3199 (9)	6.0 (3)
		R(3)		
C(1)	0.1433 (5)	−0.1044 (11)	−0.3573 (7)	5.1 (2)
C(2)	0.1425 (6)	0.0356 (10)	−0.3611 (7)	4.1 (3)
C(3)	0.1447 (7)	0.1104 (11)	−0.2825 (8)	3.2 (2)
C(4)	0.1476 (6)	0.0453 (12)	−0.2000 (7)	4.3 (3)
C(5)	0.1483 (6)	−0.0947 (12)	−0.1963 (8)	5.4 (3)
C(6)	0.1462 (6)	−0.1695 (11)	−0.2749 (8)	5.4 (3)
		R(4)		
C(1)	0.1753 (5)	0.3559 (11)	−0.1946 (8)	3.5 (3)
C(2)	0.1554 (6)	0.4772 (12)	−0.1640 (7)	3.8 (2)
C(3)	0.1875 (5)	0.5445 (12)	−0.0929 (9)	4.9 (3)
C(4)	0.2394 (5)	0.4907 (11)	−0.0522 (8)	5.1 (3)
C(5)	0.2593 (6)	0.3695 (12)	−0.0827 (7)	4.7 (3)
C(6)	0.2272 (5)	0.3021 (11)	−0.1539 (8)	4.1 (3)

Table VIII. Principal Intramolecular Distances and Angles for the $[Ni_2(tren)_2(O_4C_6Cl_2)]^{2+}$ Cation

Distances, Å			
Ni-O(1)	2.130 (3)	C(3)-Cl	1.731 (5)
Ni-O(2)	2.044 (3)	N(1)-C(4)	1.493 (7)
Ni-N(1)	2.085 (4)	C(4)-C(5)	1.502 (8)
Ni-N(2)	2.109 (4)	N(2)-C(5)	1.474 (6)
Ni-N(3)	2.058 (4)	N(1)-C(6)	1.489 (6)
Ni-N(4)	2.141 (5)	C(6)-C(7)	1.530 (8)
O(1)-C(1)	1.265 (5)	N(3)-C(7)	1.467 (6)
O(2)-C(2)	1.251 (5)	N(1)-C(8)	1.479 (7)
C(1)-C(2)	1.536 (6)	C(8)-C(9)	1.509 (10)
C(2)-C(3)	1.391 (6)	N(4)-C(9)	1.483 (8)
C(1)-C(3)′	1.381 (6)	O(1)···O(2)	2.619 (5)
Angles, Deg			
O(1)-Ni-O(2)	77.7 (1)	O(1)-C(1)-C(3)′	125.1 (4)
O(1)-Ni-N(1)	105.5 (1)	O(2)-C(2)-C(3)	124.7 (4)
O(1)-Ni-N(2)	83.8 (2)	C(1)-C(2)-C(3)	119.6 (4)
O(1)-Ni-N(3)	170.6 (1)	C(2)-C(3)-C(1)′	120.5 (4)
O(1)-Ni-N(4)	85.3 (2)	C(2)-C(1)-C(3)′	119.8 (4)
O(2)-Ni-N(1)	174.9 (2)	C(2)-C(3)-Cl	118.9 (4)
O(2)-Ni-N(2)	101.1 (2)	C(1)-C(3)′-Cl′	121.0 (4)
O(2)-Ni-N(3)	93.5 (1)	Ni-N(1)-C(4)	106.4 (3)
O(2)-Ni-N(4)	94.5 (2)	Ni-N(1)-C(6)	109.4 (3)
N(1)-Ni-N(2)	83.3 (2)	Ni-N(1)-C(8)	105.8 (3)
N(1)-Ni-N(3)	83.5 (2)	Ni-N(2)-C(5)	108.8 (3)
N(1)-Ni-N(4)	81.9 (2)	Ni-N(3)-C(7)	107.2 (3)
N(2)-Ni-N(3)	95.1 (2)	Ni-N(4)-C(9)	110.1 (4)
N(2)-Ni-N(4)	158.5 (2)	N(1)-C(4)-C(5)	109.8 (4)
N(3)-Ni-N(4)	98.5 (2)	N(2)-C(5)-C(4)	108.8 (5)
Ni-O(1)-C(1)	114.0 (3)	N(1)-C(6)-C(7)	112.1 (4)
Ni-O(2)-C(2)	117.2 (3)	N(3)-C(7)-C(6)	108.8 (4)
O(1)-C(1)-C(2)	115.2 (4)	N(1)-C(8)-C(9)	110.3 (5)
O(2)-C(2)-C(1)	115.7 (4)	N(4)-C(9)-C(8)	109.2 (5)

carbonyl infrared bands above 1600 cm^{-1} indicate a localized electronic structure for chloranilate ligand. The structural features of the bridging chloranilate ligand in $[Ni_2(tren)_2(CA)]^{2+}$ are more similar to those found for the free dianion. Both are essentially planar with delocalization confined to upper and lower regions of the ring as illustrated below. The

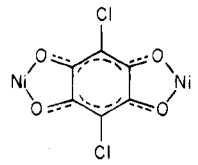

C(1)–C(2) length of 1.536 (6) Å in the present structure and 1.535 (8) Å for the chloranilate ion[21] indicate little conjugation between halves of the ligand. The chloranilate bridge, therefore, bears a qualitative resemblance to bridged oxalate complexes where the carbon–carbon bond between upper and lower regions of the bridge is not involved with conjugation and is of single bond order. For comparison, the oxalate C–C bond in $[Cu_2(Et_5dien)_2(oxalate)](BPh_4)_2$ is 1.53 (1) Å.[1] Squarate-bridged complexes may undergo complete delocalization over the ring, although a length of 1.487 (16) Å has been reported for the C–C bond within the chelate ring of the magnetically coupled polymer $[Ni(H_2O)_2(O_4C_4)]_n$.[30] Carbon–oxygen lengths within the Ni–chloranilate chelate ring of 1.251 (5) and 1.265 (5) Å are longer than lengths of 1.237 (7) Å found in $[Ni_2(en)_4(oxalate)]^{2+}$[31] and 1.222 (14) Å in $[Ni(H_2O)_2(O_4C_4)]_n$.

The Ni–O lengths of 2.044 (3) and 2.130 (3) Å in $[Ni_2(tren)_2(CA)]^{2+}$ differ significantly but average to a value compatible with the 2.060 (9) Å Ni–O length in the squarate-bridged $[Ni(H_2O)_2(O_4C_4)]_n$ and values of 2.093 (4) and 2.097 (4) Å in $[Ni_2(en)_4(oxalate)]^{2+}$. Unsymmetrical bridges were also observed in $[Ni_2(tren)_2(N_3)_2]^{2+}$ and $[Ni_2(tren)_2(NCO)_2]^{2+}$, which have end-to-end bridging azide[32] and cyanate[33] ions. While differences in Ni–O and Ni–N lengths for the dicyanate bridge in $[Ni_2(tren)_2(NCO)_2]^{2+}$ may be expected, the magnitude of the difference between Ni–O lengths for the chloranilate bridge and between Ni–N distances (2.069 (8) and 2.195 (7) Å) in the diazido bridge of $[Ni_2(tren)(N_3)_2]^{2+}$ is somewhat surprising. The unsymmetrical bridging in the three Ni–tren structures is probably a consequence of two effects. First, the strong tendency of Ni(II) to be octahedral played against the tendency of the tren ligand to enforce a trigonal-bipyramidal structure is important. Other first-row metal–tren complexes known to be trigonal bipyramidal are $[Cu(tren)X](BPh_4)$,[34,35] where $X^- = CN^-$, NCO^-, NCS^-, and Cl^-, $[Mn(tren)X](BPh_4)$,[36] where $X^- = NCO^-$ and NCS^-, and $[Zn(tren)Cl](BPh_4)$.[37] The second effect is related to the difference in donor activity of the primary and tertiary amine nitrogen atoms of the tren ligand and their influence on donor bonding at trans positions. In all three binuclear Ni–tren complexes the central tren nitrogen atom is more weakly bound than the primary nitrogen atom in the bridge plane of the octahedron. In each case the weakest Ni–X bond of the bridge occurs at the site trans to the primary amine nitrogen. However, the differences in Ni–N lengths for the two types of amine nitrogen atoms is substantially smaller than differences in Ni–X lengths of the bridge.

Structure of $[Cu_2(Me_5dien)_2(CA)](BPh_4)_2$. As was found for the nickel complex, the structure of the copper chloranilate compound shows discrete BPh_4^- anions and chloranilate-bridged dimeric cations, $[Cu_2(Me_5dien)_2(CA)]^{2+}$. Table X lists the principal intramolecular bonding parameters for the $[Cu_2(Me_5dien)_2(CA)]^{2+}$ cation. An ORTEP plot of the dimeric cation is illustrated in Figure 2. As can be seen, the chloranilate dianion bridges the two copper ions in a bis bidentate fashion. The Cu–Cu distance in the centrosymmetric dimer is calculated to be 7.858 (2) Å. The chloranilate bridge is planar, and the two copper ions lie 0.145 Å out of this plane; see Table XI. The dimensions of the chloranilate ligand in $[Cu_2(Me_5dien)_2(CA)](BPh_4)_2$ are the same within experimental error as those of $[Ni_2(tren)_2(CA)](BPh_4)_2$. The copper compound also has a partially delocalized, quinoid chloranilate bridge.

The geometry about the copper ion is best described as intermediate between a trigonal bipyramid and a square pyramid. Viewing the structure as a square pyramid, oxygen atom O(2) occupies the apical position with O(1) and the nitrogen donors in the basal plane. The trans angle for O(1) and N(2) is linear (177.3 (2)°); however, the positions of N(1) and N(3) are well below the idealized basal plane. Nitrogens N(1) and N(3) with O(2) define the equatorial plane of the molecule in the distorted trigonal bipyramidal view of the

Table IX. Deviations from the Chloranilate Least-Squares Plane for $[Ni_2(tren)_2(O_4C_6Cl_2)](B(C_6H_5)_4)_2$

Plane:[a] $5.67x + 1.63y - 21.52z = 2.80$

Atom	Distance, Å	Atom	Distance, Å
O(1)	0.025 (4)	Cl	0.004 (2)
O(2)	−0.013 (3)	Ni	−0.029
C(1)	−0.007 (5)	N(1)	0.095
C(2)	−0.021 (6)	N(3)	−0.188
C(3)	−0.031 (5)		

[a] Least-squares plane is in crystal coordinates as defined by W. C. Hamilton, *Acta Crystallogr.*, **18**, 502 (1965).

Table X. Principal Intramolecular Bonding Parameters for the $[Cu_2(Me_5dien)_2(O_4C_6Cl_2)]^{2+}$ Cation

Distances, Å

Cu-O(1)	1.956 (4)	N(1)-C(4)	1.477 (10)
Cu-O(2)	2.196 (4)	N(1)-C(8)	1.465 (10)
Cu-N(1)	2.037 (6)	N(1)-C(9)	1.477 (10)
Cu-N(2)	1.988 (5)	N(2)-C(5)	1.463 (10)
Cu-N(3)	2.045 (6)	N(2)-C(6)	1.495 (10)
O(1)-C(1)	1.257 (7)	N(2)-C(10)	1.504 (10)
O(2)-C(2)	1.245 (7)	N(3)-C(7)	1.479 (9)
C(1)-C(2)	1.542 (8)	N(3)-C(11)	1.473 (9)
C(2)-C(3)	1.382 (8)	N(3)-C(12)	1.483 (10)
C(1)-C(3)′	1.380 (8)	C(4)-C(5)	1.458 (12)
C(3)-Cl	1.736 (6)	C(6)-C(7)	1.475 (12)
		O(1)···O(2)	2.644 (6)

Angles, Deg

O(1)-Cu-O(2)	78.9 (2)	O(2)-C(2)-C(1)	115.6 (5)
O(1)-Cu-N(1)	93.3 (2)	O(2)-C(2)-C(3)	125.6 (6)
O(1)-Cu-N(2)	177.3 (2)	C(1)-C(3)′-C(2)′	122.8 (5)
O(1)-Cu-N(3)	92.3 (2)	C(2)-C(3)-Cl	119.3 (4)
O(2)-Cu-N(1)	106.0 (2)	C(1)′-C(3)-Cl	117.9 (5)
O(2)-Cu-N(2)	103.7 (2)	Cu-N(1)-C(4)	105.4 (5)
O(2)-Cu-N(3)	102.1 (2)	N(1)-C(4)-C(5)	111.8 (8)
N(1)-Cu-N(2)	86.7 (2)	C(4)-C(5)-N(2)	111.3 (7)
N(1)-Cu-N(3)	151.8 (2)	Cu-N(2)-C(5)	108.0 (4)
N(2)-Cu-N(3)	86.4 (2)	Cu-N(2)-C(6)	105.3 (4)
Cu-O(1)-C(1)	117.7 (4)	C(5)-N(2)-C(6)	113.0 (6)
Cu-O(2)-C(2)	110.8 (4)	N(2)-C(6)-C(7)	109.8 (6)
O(1)-C(1)-C(2)	116.7 (5)	C(6)-C(7)-N(3)	109.5 (6)
O(1)-C(1)-C(3)′	124.9 (6)	Cu-N(3)-C(7)	107.1 (5)

Table XI. Least-Squares Planes for $[Cu_2(Me_5dien)_2(O_4C_6Cl_2)](B(C_6H_5)_4)_2$

Atom	Distance, Å	Atom	Distance, Å
Chloranilate Plane: $15.63x + 4.49y - 10.20z = -0.05$			
Cl	0.002 (2)	Cu	0.145
C(1)	−0.006 (7)	N(2)	0.311
C(2)	−0.011 (6)	O(1)	0.012 (5)
C(3)	−0.010 (6)	O(2)	−0.006 (5)
Basal Plane: $5.48x - 9.11y - 5.31z = 2.50$			
N(1)	−0.269 (7)	O(1)	0.129 (5)
N(2)	0.272 (7)	Cu	0.245
N(3)	−0.201 (6)		

geometry. The bite angle of 78.9 (2)° for the chloranilate chelate ring and the dien N–Cu–N angles of 86.4 (2) and 86.7 (2)° tip the equatorial plane out of the idealized position normal to the axial bonds. Bonds Cu–O(1) and Cu–N(2) form angles of 78.8 (3) and 76.1 (3)° with the N(1), N(3), O(2) plane.

The ambiguous geometry of the complex relates directly to the value of the N(1)–Cu–N(3) bond angle, which would be 120 or 180° in the two regular five-coordinate polyhedra but is found to be 151.8 (2)°. Two related oxalate-bridged complexes $[Cu_2(dien)_2(C_2O_4)]^{2+}$ and $[Cu_2(Et_5dien)_2(C_2O_4)]^{2+}$ have been examined structurally,[1,31] and their features appear to indicate that the distortion of $[Cu_2(Me_5dien)_2(CA)]^{2+}$ from a square-pyramidal geometry is steric in origin. In all three structures the central dien nitrogen and one oxygen donor have a bond angle close to 180°. Of this series, $[Cu_2(Et_5dien)_2(C_2O_4)]^{2+}$ with bulky ethyl substituents has the geometry closest to a regular trigonal bipyramid. Bond angles in the trigonal plane are 97.5 (2) and 131.1 (2)° for the N–Cu–O angles and 131.4 (2)° for the N–Cu–N angle. Related bond angles in $[Cu_2(dien)_2(C_2O_4)]^{2+}$ are 99 (1)° for the O–Cu–N angles and 160.3 (7)° for N–Cu–N angle. This suggests that in the absence of steric interactions created by dien substituents a square-pyramidal geometry is preferred. With substituents of intermediate size in $[Cu_2(Me_5dien)_2(CA)]^{2+}$ bond angles of 102.1 (2), 106.0 (2), and 151.8 (2)° are observed. The progressive change in geometry through this series is also reflected in the Cu–O length at the "apical" position. For $[Cu_2(dien)_2(C_2O_4)]^{2+}$ this length is 2.230 (6) Å, $[Cu_2(Me_5dien)_2(CA)]^{2+}$ shows an intermediate value of 2.196 (4) Å, while in the trigonal plane of $[Cu_2(Et_5dien)_2(C_2O_4)]^{2+}$ the value is 2.174 (4) Å. Other Cu–O lengths for the three structures fail to show this consistency with the Cu–O(1) length of 1.956 (4) Å for the present structure the shortest of the series.

Magnetic Susceptibility of Ni(II) Dimers. In addition to the chloranilate-bridged Ni(II) compound, two other related dimeric Ni(II) compounds were prepared: $[Ni_2(tren)_2(DHBQ)](BPh_4)_2$ and $[Ni_2(tren)_2(RHZ)](BPh_4)_2$. We are certain that the $DHBQ^{2-}$ compound is isostructural with the chloranilate compound, because early in this study x-ray diffraction data were collected for the $DHBQ^{2-}$ compound and similar results (i.e., space group and dimer Ni–Ni distance) were obtained. Crystal decomposition during data collection led to the discontinuance of structural work on this compound. It also seems very reasonable that the rhodizonate compound, $[Ni_2(tren)_2(RHZ)](BPh_4)_2$, would have the same basic structure. However, the rhodizonate dianion II can conceivably bridge two Ni(II) ions in two different ways.

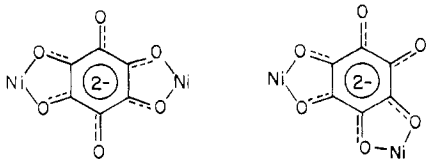

All three nickel compounds have 4.2–270 K magnetic susceptibility curves that are characteristic of an antiferromagnetic exchange interaction. Experimental and theoretical fit data are given in Tables XII–XIV.[22] The three curves are very similar; Figure 4 illustrates the data obtained for $[Ni_2(tren)_2(DHBQ)](BPh_4)_2$. As can be seen in Figure 4, the molar paramagnetic susceptibility (χ_M) for the dimer continues to increase with decreasing temperature down to 4.2 K. The μ_{eff} at 270 K is 3.15 μ_B per Ni(II) ion and this decreases gradually down to ~20 K whereupon the μ_{eff} value decreases more rapidly with decreasing temperature down to 1.97 μ_B per Ni(II) ion at 4.2 K, a behavior which is characteristic of an antiferromagnetic exchange interaction. The susceptibility

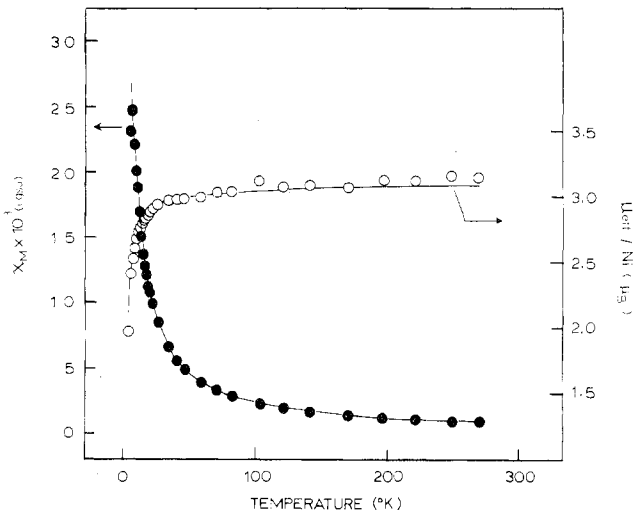

Figure 4. Corrected molar paramagnetic susceptibility (χ_M in cgsu per dimer) and effective magnetic moment per nickel ion (μ_{eff}/Ni in μ_B) vs. temperature curves for $[Ni_2(tren)_2(DHBQ)](BPh_4)_2$. The experimental data are represented as circles and the lines result from a least-squares fit to theoretical equations with $J = -1.1$ cm^{-1}, $g = 2.17$, $D = 4.4$ cm^{-1}, and $Z'J' = -0.0076$ cm^{-1}.

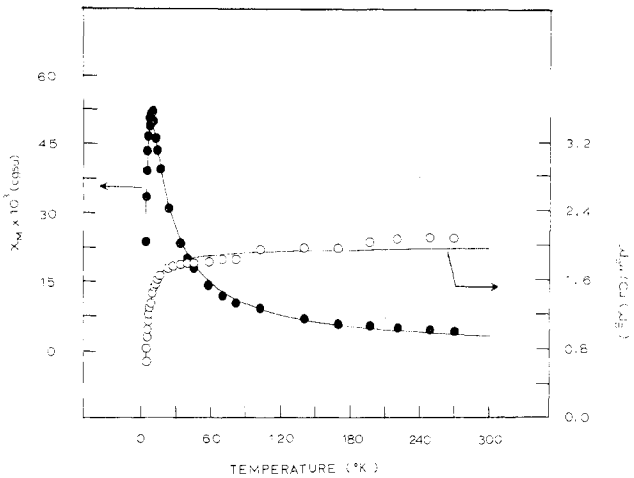

Figure 5. Corrected molar paramagnetic susceptibility (χ_M in cgsu per dimer) and effective magnetic moment per copper ion (μ_{eff}/Cu in μ_B) vs. temperature curves for $[Cu_2(dpt)_2(DHBQ)](BPh_4)_2$. The experimental data are represented as circles and the lines result from a least-squares fit to theoretical equations with $J = -4.6$ cm^{-1}, $g = 2.25$, and $\Theta = -1.1°$.

data were least-squares fit to the theoretical equations derived by Ginsberg et al.[38] for an isotropic exchange interaction ($\hat{H} = -2J\hat{S}_1\cdot\hat{S}_2$ with exchange parameter J) in a dimeric nickel(II) complex. The equations account for single-ion zero-field interactions (represented by the parameter D) and *inter*dimer interactions (represented by the effective interdimer exchange parameter $Z'J'$). As shown in Figure 4, a very reasonable least-squares fit of the data (points) for $[Ni_2(tren)_2(DHBQ)](BPh_4)_2$ was obtained as represented by the solid lines. The fitting parameters were found to be $J = -1.1$ cm^{-1}, $g = 2.17$, and $D = 4.4$ cm^{-1}. The *inter*dimer effective exchange parameter, $Z'J'$, was found to fit at a negligible value of -0.0076 cm^{-1}. It is not possible to determine the sign of the single-ion zero-field splitting parameter D, because an equally good fit is obtained with $D = -4.4$ cm^{-1} where the other parameters remain the same.

At 270 K, μ_{eff} per Ni(II) ion for $[Ni_2(tren)_2(CA)](BPh_4)_2$ is 3.43 μ_B and this decreases to 1.79 μ_B for 4.2 K. Least-squares fitting of the data for this compound gives $J = -1.8$

cm^{-1}, $g = 2.30$, $|D| = 3.8$ cm^{-1}, and $Z'J' = -0.0069$ cm^{-1}. As is indicated by the smaller value of μ_{eff} at 4.2 K, the chloranilate compound exhibits a somewhat greater antiferromagnetic interaction than the 2,5-dihydroxy-1,4-benzoquinone compound. The difference in exchange parameters is not large, however.

The rhodizonate dianion II is *not* expected to be isostructural with the dianions from the 2,5-dihydroxy-1,4-benzoquinones. In the previous sections the structures of these latter dianions were shown to be quinonoid, that is, partially delocalized. As far as we know, there is no report of structural work on any rhodizonate compound. Molecular orbital calculations on the rhodizonate dianion indicate an aromatic delocalized structure where all the C–C bond lengths are equal.[39] The magnetic susceptibility data for $[Ni_2(tren)_2(RHZ)](BPh_4)_2$ are listed in Table XIV.[22] The μ_{eff}/Ni value ranges from 3.21 μ_B at 270 K to 1.84 μ_B at 4.2 K. Least-squares fitting to the theoretical equations gives $J = -3.9$ cm^{-1}, $g = 2.10$, $|D| = -3.4$ cm^{-1}, and $Z'J' = -0.0074$ cm^{-1}. The fit is not as good as those obtained for the other two nickel compounds, which probably means that the J value for the rhodizonate compound is the least accurately known. The greatest deviation between the theoretical curve and the experimental data occurs below ~10 K. This could be explained by the presence of a paramagnetic impurity.

Magnetic Susceptibility and Electron Paramagnetic Resonance of Cu(II) Dimers. In addition to $[Cu_2(Me_5dien)_2(CA)](BPh_4)_2$, the compounds $[Cu_2(Me_5dien)_2(DHBQ)](BPh_4)_2$, $[Cu_2(dpt)_2(CA)](BPh_4)_2$, and $[Cu_2(dpt)_2(DHBQ)](BPh_4)_2$ were prepared. Variable-temperature magnetic susceptibility data for these four compounds are collected in Tables XV–XVIII.[22] There is no evidence of an exchange interaction in the data for either of the Me_5dien compounds, whereas, the two dpt compounds are clearly involved in antiferromagnetic exchange interactions.

The data for $[Cu_2(dpt)_2(DHBQ)](BPh_4)_2$ are illustrated in Figure 5, where it can be seen that the molar paramagnetic susceptibility, χ_M, shows a maximum at ~9.5 K. The μ_{eff} per Cu(II) ion starts at 2.08 μ_B at 270 K and decreases to 0.63 μ_B at 4.2 K. The susceptibility data for this compound were least-squares fit to the Bleaney–Bowers equation[40] for isotropic exchange in a Cu(II) dimer

$$\chi_M = \frac{Ng^2\beta^2}{k(T-\Theta)}\left[\frac{2}{3+\exp(-2J/kT)}\right] + N\alpha$$

The temperature-independent paramagnetism, $N\alpha$, for a Cu(II) dimer was taken as 120×10^{-6} cgsu per mole of dimer. In the above equation, then, there are three parameters, J, g, and the Weiss constant Θ, which treat *inter*dimer interactions.[41] Least-squares fitting the data for $[Cu_2(dpt)_2(DHBQ)](BPh_4)_2$ gives $J = -4.6$ cm^{-1}, $g = 2.25$, and $\Theta = -1.1°$. In the least-squares fitting of a weakly antiferromagnetic compound, the g value is determined by the high-temperature susceptibilities. The J value that is obtained is *not* very affected by small changes (±0.1) in the g value. It would have been best to use the g value from the EPR spectrum in the fitting. The Q-band EPR spectrum of $[Cu_2(dpt)_2(DHBQ)](BPh_4)_2$ shows a rhombic signal with no copper hyperfine visible and g values of 2.016, 2.136, and 2.233, which gives an average g value of 2.128 from the EPR spectrum. It is not clear why the average g value from the susceptibility differs so much. In passing it is to be noted that the Q-band EPR spectrum of $[Cu_2(dpt)_2(oxalate)](BPh_4)_2$ is similar in appearance; however, the intermediate field resonance is at higher field; g values are 2.032, 2.074, and 2.236 with an average g value of 2.114.[1] The copper coordination geometries of both of these compounds are probably distorted trigonal bipyramids, as indicated by a g value close to 2.00.[42] It appears that the coordination geometry in $[Cu_2(dpt)_2(DHBQ)](BPh_4)_2$ is closer to an idealized trigonal bipyramid, because the g values better mimic those reported[34] for $Cu(tren)X^+$ species.

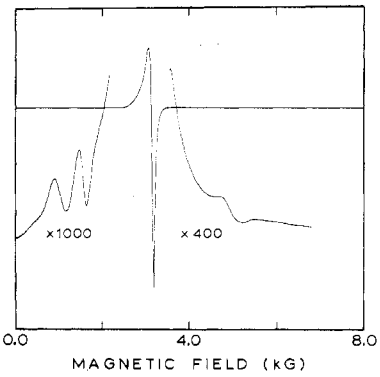

Figure 6. X-Band (9.1566 GHz) EPR spectrum of a powdered sample of $[Cu_2(Me_5dien)_2(DHBQ)](BPh_4)_2$ at ~9 K.

The μ_{eff}/Cu varies from 2.04 μ_B at 249 K to 0.87 μ_B at 4.2 K for $[Cu_2(dpt)_2(CA)](BPh_4)_2$. The susceptibility peaks at ~4.7 K. Least-squares fitting of the data gives $J = -2.0$ cm^{-1}, $g = 2.25$, and $\Theta = -5.0°$. The Q-band EPR spectrum (g = 2.018, 2.123, and 2.240) is almost identical with that for the $DHBQ^{2-}$ compound. Again there is no copper hyperfine seen in the spectrum.

In view of the fact that $[Cu_2(Me_5dien)_2(CA)](BPh_4)_2$ contains chloranilate-bridged Cu(II) dimers, $[Cu_2(Me_5dien)_2(CA)]^{2+}$, it was somewhat puzzling to find that the magnetic susceptibility data to 5.3 K gave little indication of an exchange interaction. The Q-band EPR spectrum of this compound maintained at either room or near-liquid-nitrogen temperature did *not* show any copper hyperfine. A very broad (300–400 G half-width) parallel signal is seen at $g = 2.203$ in conjunction with a "shouldered" derivative at $g = 2.053$.

The compound $[Cu_2(Me_5dien)_2(DHBQ)](BPh_4)_2$ also shows no signs of an exchange interaction with susceptibility data to 4.7 K. The Q-band EPR spectrum is very similar to that for the corresponding chloranilate compound.

No indication of an exchange interaction in magnetic susceptibility measurements taken to a low temperature of ~5 K means that $|J| < \sim 0.5$ cm^{-1} for a copper dimer. If the exchange parameter J is less than the energy of the microwave radiation used in an EPR experiment (~0.3 cm^{-1} for X-band), then it is sometimes possible to see EPR transitions between the singlet electronic state of a copper dimer and the $\Delta M_s = \pm 1$ components of the triplet state. There are two transitions and these singlet-to-triplet transitions are forbidden and, as such, of low intensity. Similar types of transitions have been seen for transition metal ions doped into extended (i.e., polymeric) compounds.[43] Only a very few copper dimers have been reported to show singlet-to-triplet EPR transitions.[44] The importance of observing such EPR transitions draws from the fact that the absolute value of the exchange parameter can be calculated from their magnetic field position. With X-band measurements $|J|$ values in the range of 0.05–0.15 cm^{-1} can be determined.

Both $[Cu_2(Me_5dien)_2(CA)](BPh_4)$ and $[Cu_2(Me_5dien)_2(DHBQ)](BPh_4)_2$ show low-intensity features in their X-band spectra. The spectrum of a powdered sample of the $DHBQ^{2-}$ compound taken at ~9 K is reproduced in Figure 6. The "normal" relatively intense $\Delta M_s = 1$ transition within the triplet state manifold is seen at ~3200 G. When the spectrometer gain is increased and the magnetic field is swept to either lower or higher field values, weaker features are seen. At lower field two weaker derivatives are seen, whereas at higher field only one is seen. The feature at ~1500 G is the so-called "half-field" $\Delta M_s = 2$ transition between the $M_s =$

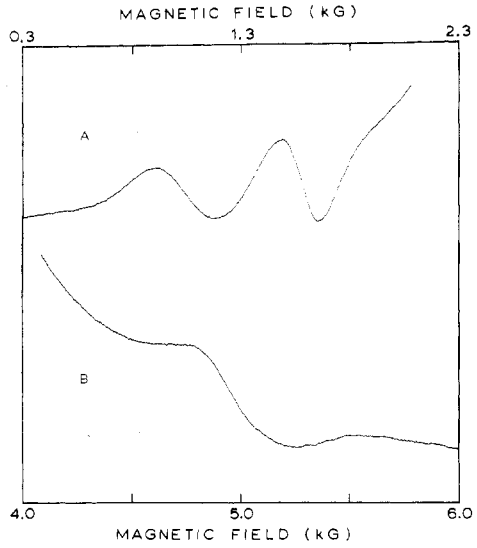

Figure 7. Expansion of low-field (A) and high-field (B) regions of the ~9 K X-band spectrum of $[Cu_2(Me_5dien)_2(DHBQ)](BPh_4)_2$.

1 and $M_s = -1$ components of the triplet state. The other two transitions can be assigned as singlet-to-triplet transitions. Each of these transitions is predicted to be at an energy of $2|J|/g\beta$ to either higher or lower field of the $\Delta M_s = 1$ transition. The observation of the two transitions is, in fact, further substantiation of their assignment. Figure 7 shows an expansion of the spectrum for the low and high fields. From the resonance positions a value of $|J|$ is calculated to be 0.1 cm^{-1} for $[Cu_2(Me_5dien)_2(DHBQ)](BPh_4)_2$. The X-band spectrum of this compound was studied as a function of temperature up to ~300 K. At temperatures above ~80 K it is difficult to resolve the two singlet-to-triplet transitions and between ~80 and ~6 K there does not seem to be much temperature dependence in the signal positions. The chloranilate compound was recrystallized from several solvents (see Experimental Section) and in each case the same weak EPR signals were seen. The compound $[Cu_2(Me_5dien)_2(CA)](BPh_4)_2$ also shows two singlet-to-triplet features in its X-band spectra; they are of somewhat poorer resolution. Within our ability to discern the resonance positions the resonances for the $DHBQ^{2-}$ compound are at the same field positions as those observed for the CA^{2-} compound.

Exchange Mechanism. Table XIX summarizes the exchange parameters for the seven compounds from this study and for several related compounds. There are two different series of copper complexes. In the case of the Me_5dien complexes, the exchange interactions for the chloranilate and 2,5-dihydroxy-1,4-benzoquinone compounds are of comparable magnitude, whereas the corresponding oxalate compound has an appreciably greater exchange interaction with an exchange parameter that is almost two orders of magnitude larger. This seems to be reasonable in naive terms, for the two hydroxy–quinone bridges are much more extended units compared to the oxalate ion. What seems to be surprising, then, is the fact that the exchange interactions for the three corresponding dpt complexes are all about the *same*. Thus, the exchange parameters for $[Cu_2(dpt)_2(DHBQ)](BPh_4)_2$ and $[Cu_2(dpt)_2(Ox)](BPh_4)_2$ are probably equal within experimental error.

An explanation for the marked variation in trends of exchange parameters noted above for the copper Me_5dien and dpt complexes can be gleaned from our previous paper.[1] A series of oxalate-bridged copper compounds with the composition $[Cu_2L_2(Ox)]X_2$, where L is variously Et_5dien, Me_5dien, dien, or dpt and X^- is BPh_4^-, ClO_4^-, or PF_6^-, was studied with magnetic and EPR techniques. The dimensions

Table XIX. Magnetic Exchange Parameters[a]

Compd	J, cm^{-1}
$[Ni_2(tren)_2(CA)](BPh_4)_2$	−1.8
$[Ni_2(tren)_2(DHBQ)](BPh_4)_2$	−1.1
$[Ni_2(tren)_2(RHZ)](BPh_4)_2$	−6.0
$[Ni_2(trien)_2(Ox)](ClO_4)_2$[b,c]	−15.6
$[Ni_2(dien)_2(H_2O)_2(Ox)](ClO_4)_2$[d]	−12.2
$[Ni_2(macro)_2(Sq)](ClO_4)_2$[b]	−0.4
$[Cu_2(Me_5dien)_2(CA)](BPh_4)_2$	0.1[e]
$[Cu_2(Me_5dien)_2(DHBQ)](BPh_4)_2$	0.1[e]
$[Cu_2(Me_5dien)_2(Ox)](BPh_4)_2$[d]	−3.4
$[Cu_2(dpt)_2(CA)](BPh_4)_2$	−2.0
$[Cu_2(dpt)_2(DHBQ)](BPh_4)_2$	−4.6
$[Cu_2(dpt)_2(Ox)](BPh_4)_2$[d]	−5.7

[a] The additional abbreviations that are used in this table are Ox for the oxalate ion $C_2O_4^{2-}$, Sq for the squarate ion $C_4O_4^{2-}$, and macro is *meso*-2,4,4,9,9,11-hexamethyl-1,5,8,12-tetraazacyclotetradecane. [b] Reference 16. [c] $[Ni_2(tren)_2(Ox)](BPh_4)_2$ gives almost identical results: see D. M. Duggan, Ph.D. Thesis, University of Illinois. [d] Reference 1. [e] Obtained from singlet-to-singlet EPR transitions and, as such, only the absolute value of the exchange parameter is known.

of the oxalate anion bridge are relatively invariant and, in spite of this, the exchange interaction for these copper compounds was found to vary from $J = -37$ cm^{-1} to a J value that did not affect the compounds susceptibility at 4.2 K (i.e., $|J| <$ ~0.5 cm^{-1}). It was shown that the two orders of magnitude variation in exchange parameter resulted from a change in local copper ion ground state. The Et_5dien complexes exhibited the strongest exchange interaction with approximately trigonal-bipyramidal copper ion coordination geometries. The complexes that most closely approximated square-pyramidal copper ion coordination geometries exhibited the weakest interactions.

The g values for the three copper Me_5dien complexes in Table XIX are close and, as such, the local copper ion coordination geometries are very similar in the three complexes. The change in J value for these Me_5dien complexes in going from the oxalate to the 2,5-dihydroxy-1,4-benzoquinone bridge is, thus, a reflection of the change in the bridge and *not* a change in copper ion ground states. On the other hand, there is a difference in g values (vide supra) for the dpt complexes and this signals a change in copper ion ground states, which explains why the exchange interaction is about the same for the three dpt complexes in Table XIX.

With the possibility of a changing copper ion ground state as a result of flexibility in coordination geometry, it is not reasonable to use the *copper* exchange parameters in Table XIX in a comparison of the magnetic exchange characteristics of Ox^{2-} and $DHBQ^{2-}$. Kobayashi et al.[14] reported that the exchange parameter between nearest-neighbor Cu^{2+} ions in polymeric Cu(DHBQ) falls in the range of −9.7 to −16.7 cm^{-1}. They assumed that the structure of polymeric Cu(DHBQ) is that of a one-dimensional lattice. This could very well not be the case, for it is known[30] that the polymer formed from Ni^{2+} and the squarate dianion is not a one-dimensional lattice. Sartene and Boutron[15] calculated an exchange parameter for two $d_{x^2-y^2}$ ground-state Cu(II) ions bridged by $DHBQ^{2-}$ and they obtained a value in the range of −15 to −26 cm^{-1}. It would be very instructive to know the structure of Cu(DHBQ) in order to evaluate if the success of the theoretical calculation is only fortuitous. It should be noted that the theoretical calculation was of the configuration interaction type. The ground state was assumed to be characterized by one unpaired electron in an orbital comprised of copper $d_{x^2-y^2}$ and $DHBQ^{2-}$ oxygen sp-hybrid functions. The exchange parameter was determined, then, by an exchange integral between the ground-state orbital (largely a $d_{x^2-y^2}$ orbital) and a π-type oxygen p_z-orbital on the $DHBQ^{2-}$ bridge.

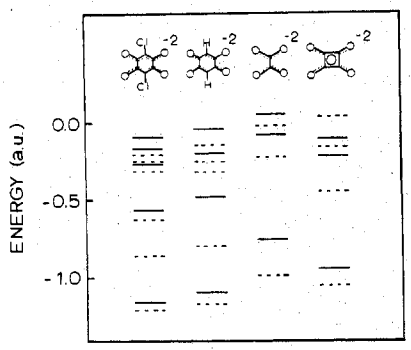

Figure 8. Occupied CNDO/2 molecular orbitals for the various dianions showing only the b_{1g} symmetry (dashed lines) and b_{2u} symmetry (solid lines) orbitals (D_{2h} point group).

The exchange parameters are summarized in Table XIX for an interesting series of nickel dimers wherein the bridge changes from oxalate ($J = -15.6$ cm^{-1}) to squarate ($J = -0.4$ cm^{-1}) to the dianion of the two 2,5-dihydroxy-1,4-benzoquinones ($J = -1.1$ and -1.8 cm^{-1}). There are two points of interest. First, the variation in exchange parameter in this series is interesting in that the J values for the dihydroxyquinones are greater than the J values for the squarate. Second, it can be seen that substituting $DHBQ^{2-}$ with two chlorine atoms to give the CA^{2-} compound leads to only a small change in the J value. A qualitative explanation of these observations will be provided.

In molecular orbital terms, the orbitals of the bridging species interact with the metal orbitals in which the unpaired electrons reside. It is the magnitude of this interaction that determines the antiferromagnetic contribution to the magnetic exchange interaction. In a nickel(II) dimer, each metal ion has two unpaired electrons, one in a d_{z^2} and the other in a $d_{x^2-y^2}$ orbital. In the dimer an interaction between the two $d_{x^2-y^2}$ orbitals (one at each metal ion) results if there are bridge orbitals of the correct symmetry and energy. Two molecular orbitals form, one that is essentially the bonding combination of $d_{x^2-y^2}$ orbitals and the other that is the antibonding combination. If the two nickel ions are designated as A and B, then the two molecular orbitals are

$$\phi_1 \simeq d^{A}_{x^2-y^2} + d^{B}_{x^2-y^2}$$

$$\phi_2 \simeq d^{A}_{x^2-y^2} - d^{B}_{x^2-y^2}$$

It has been shown[45] that the difference in energy between these two molecular orbitals for the dimer determines the magnitude of the antiferromagnetic interaction. With a nickel(II) dimer it is also necessary to consider the interaction of the d_{z^2} metal orbitals as propagated by the bridge orbitals. However, there would not be nearly as strong an interaction of the d_{z^2} orbitals with the bridge orbitals as for the $d_{x^2-y^2}$ orbitals in the nickel dimer, because the main lobes of the d_{z^2} metal orbitals are for the most part directed perpendicular to the plane of the bridging species. Approximate calculations[45] support the supposition that the d_{z^2} orbitals are involved in a weaker interaction. Thus, the antiferromagnetic interactions in our series of nickel dimers will approximately parallel the energy difference between the above ϕ_1 and ϕ_2 orbitals.

The bridges in the nickel dimers are planar and, as such, each dimer can be assumed to have essentially D_{2h} symmetry where the bridge plane is taken as the xy plane and the Ni–Ni vector as the x axis. In the D_{2h} point group the ϕ_1 orbital has b_{2u} symmetry and the ϕ_2 orbital has b_{1g} symmetry. CNDO/2 molecular orbital calculations were carried out for each of the dianionic bridges. In Figure 8 are summarized the relative energies of the b_{2u} and b_{1g} symmetry molecular orbitals of the bridge species. These are the orbitals that interact with the

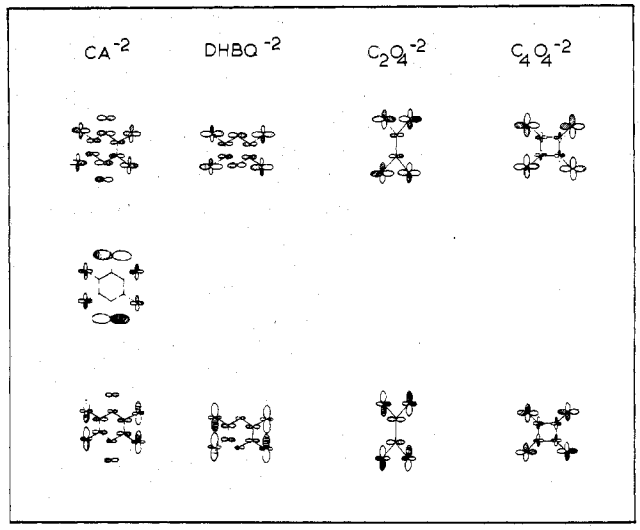

Figure 9. Sketches of the two or three highest occupied b_{1g} symmetry molecular orbitals for the dianions. The highest energy b_{1g} orbitals are pictured in the top row whereas the second highest b_{1g} orbitals are pictured in the bottom row. The chloranilate dianion has a third b_{1g} orbital which has an energy intermediate between these two.

metal $d_{x^2-y^2}$ orbitals. The magnitude of the antiferromagnetic exchange interaction present in a particular dimer depends on various factors: (1) the overlap between the $d_{x^2-y^2}$ orbital and the bridge molecular orbitals, (2) the energy difference between the $d_{x^2-y^2}$ orbital and the bridge molecular orbitals. In viewing Figure 8 it is important to remember that the d orbitals lie at higher energies than do the bridge orbitals. The metal $d_{x^2-y^2}$ orbitals interact with the b_{2u} and b_{1g} orbitals and the ϕ_1 and ϕ_2 combinations are displaced to somewhat higher energies than the starting energy of the $d_{x^2-y^2}$ orbitals. A careful examination of the b_{1g} and b_{2u} bridge orbitals leads to one very important conclusion: the b_{1g} bridge orbitals interact with the metal $d_{x^2-y^2}$ orbitals to a much greater degree than the b_{2u} orbitals do (again substantiated by calculations[45]).

We are now in a position to offer a qualitative explanation for the trends in exchange parameters observed for the nickel dimers. As can be seen from Figure 8 and the details of the b_{1g} molecular orbitals, the approximately equal exchange parameters for $[Ni_2(tren)_2(DHBQ)](BPh_4)_2$ and $[Ni_2(tren)_2(CA)](BPh_4)_2$ result from the fact that the compositions and energies of the b_{1g} orbitals for the two dianionic bridges are very similar. The CA^{2-} bridge does have one additional b_{1g} orbital at -4.57 eV, but this orbital is essentially comprised of chlorine p_x orbitals with little potential for interacting with the metal $d_{x^2-y^2}$ orbitals. The highest energy b_{1g} orbitals of the various bridging dianions are sketched in Figure 9.

As we suggested earlier,[16] and Hoffmann et al.[45] supported with extended Hückel MO calculations, the oxalate ion leads to a greater antiferromagnetic interaction between two nickel ions than the squarate ion because the highest occupied oxalate b_{1g} orbitals are at higher energy than those for the squarate ion. This leads to a greater interaction of the oxalate b_{1g} orbitals with the metal $d_{x^2-y^2}$ orbitals and, as a consequence, a greater antiferromagnetic interaction.

The two 2,5-dihydroxy-1,4-benzoquinone dianions apparently support a slightly better antiferromagnetic interaction than the squarate dianion because there are more b_{1g} exchange pathways and because the quinone b_{1g} orbitals are at slightly higher energy than the corresponding squarate orbitals.

In closing it is noted that the rhodizonate dianion has a similar b_{1g} distribution as do the quinone dianions. In separate CNDO/2 calculations it was found that the rhodizonate dianion is most stable in the aromatic delocalized form. In one rhodizonate calculation, two C–C bonds were taken as

1.536 Å and the other four as 1.386 Å. In another calculation all six C–C bonds were taken as 1.436 Å. The later symmetrical form is found to be more stable with a difference in total electronic energies between the two forms of 1.37 eV (= 31.6 kcal/mol).

Acknowledgment. C.G.P. wishes to thank Mr. R. C. Haltiwanger for help with data collection and the University of Colorado Computing Center for a generous allocation of computational time. D.N.H. and L.C.F. thank Mr. T. R. Felthouse for some assistance with experimental work. We are grateful for support from National Institutes of Health Grant HL 13652 (to D.N.H.).

Registry No. $[Ni_2(tren)_2(CA)](BPh_4)_2$, 63301-72-4; $[Ni_2(tren)_2(DHBQ)](BPh_4)_2$, 63301-74-6; $[Ni_2(tren)_2(RHZ)](BPh_4)_2$, 63428-49-9; $[Cu_2(Me_5dien)_2(CA)](BPh_4)_2$, 63301-84-8; $[Cu_2(Me_5dien)_2(DHBQ)](BPh_4)_2$, 63301-76-8; $[Cu_2(dpt)_2(DHBQ)](BPh_4)_2$, 63340-24-9; $[Cu_2(dpt)_2(CA)](BPh_4)_2$, 63301-78-0.

Supplementary Material Available: Tables I (analytical data) and XII–XVIII (experimental and calculated magnetic susceptibility data for the three nickel–tren compounds, the two copper–dpt compounds, and the two copper–Me_5dien compounds, respectively) and final values of $10|F_o|$ and $10|F_c|$ for both $[Ni_2(tren)_2(CA)](BPh_4)_2$ and $[Cu_2(Me_5dien)_2(CA)](BPh_4)_2$ (54 pages). Ordering information is given on any current masthead page.

References and Notes

(1) Part 10: T. R. Felthouse, E. J. Laskowski, and D. N. Hendrickson, *Inorg. Chem.*, **16**, 1077 (1977).
(2) University of Colorado.
(3) University of Illinois.
(4) Camille and Henry Dreyfus Fellow, 1972–1977; A. P. Sloan Foundation Fellow, 1976–1978.
(5) (a) S. Patai, Ed., "The Chemistry of the Quinonoid Compounds", Parts 1 and 2, Wiley, 1974; (b) R. H. Thompson, "Naturally Occurring Quinones", 2nd ed, Academic Press, New York, N.Y., 1971; (c) M. Schnitzer and S. U. Khan, "Humic Substances in the Environment", Marcel Dekker, New York, N.Y., 1972.
(6) (a) R. M. Williams and S. C. Wallwork, *Acta Crystallogr.*, **23**, 448 (1967); (b) B. Kamenar, C. K. Prout, and J. D. Wright, *J. Chem. Soc.*, 4851 (1965).
(7) G. N. Schrauzer and H. Thyret, *J. Am. Chem. Soc.*, **82**, 6420 (1960).
(8) C. G. Pierpont and H. H. Downs, submitted for publication in *Inorg. Chem.*
(9) C. G. Pierpont and H. H. Downs, *J. Am. Chem. Soc.*, **97**, 2123 (1975).
(10) A. A. Vlček and J. Hanslik, *Inorg. Chem.*, **6**, 2053 (1967).
(11) C. Floriani, G. Fachinetti, and F. Calderazzo, *J. Chem. Soc., Dalton Trans.*, 765 (1973).
(12) M. A. A. Beg, *Pak. J. Sci. Ind. Res.*, **14**, 452 (1971), and references therein.
(13) H. D. Coble and H. F. Holtzclaw, Jr., *J. Inorg. Nucl. Chem.*, **36**, 1049 (1974).
(14) H. Kobayashi, T. Haseda, E. Kanda, and S. Kanda, *J. Phys. Soc. Jpn.*, **18**, 349 (1963).
(15) R. Sartene and F. H. Boutron, *Mol. Phys.*, **18**, 825 (1970).
(16) D. M. Duggan, E. K. Barefield, and D. N. Hendrickson, *Inorg. Chem.*, **12**, 985 (1973).
(17) D. M. Duggan and D. N. Hendrickson, *Inorg. Chem.*, **12**, 2422 (1973).
(18) G. R. Hall, D. M. Duggan, and D. N. Hendrickson, *Inorg. Chem.*, **14**, 1956 (1975).
(19) E. K. Andersen, *Acta Crystallogr.*, **22**, 188 (1967).
(20) S. Kulpe and S. Dähne, *Tetrahedron Lett.*, **21**, 2591 (1968).
(21) E. K. Andersen, *Acta Crystallogr.*, **22**, 196 (1967).
(22) Supplementary material.
(23) B. N. Figgis and J. Lewis in "Modern Coordination Chemistry", J. Lewis and R. G. Wilkins, Ed., Interscience, New York, N.Y., 1960, p 403; P. W. Selwood, "Magnetochemistry", 2nd ed, Interscience, New York, N.Y., 1956, pp 78, 92, 93.
(24) J. P. Chandler, Program 66, Quantum Chemistry Program Exchange, Indiana University, Bloomington, Ind., 1973.
(25) The following programs were used for crystallographic calculations: CUPROC, a local data processing program; NUCLS, Ibers' group least-squares program; FORDAP, Zalkin's Fourier program; ORFFE, the Busing–Levy function and error program; ORTEP, Johnson's graphics program. Lorentz and polarization corrections were calculated by the formula

$$Lp = \frac{1}{\sin 2\theta}\left[F\left(\frac{\cos^2 2\theta_m + \cos^2 2\theta}{1 + \cos^2 2\theta_m}\right) + (1-F)\left(\frac{\cos 2\theta_m + \cos^2 2\theta}{1 + \cos 2\theta_m}\right)\right]$$

where F is the fraction of mosaic character associated with the monochromator crystal and was set equal to 0.5. Standard deviations were calculated by the equation

$$\sigma(I) = [CT + 0.25T^2(B_1 + B_2) + (PI)^2]^{1/2}$$

where CT = total integrated peak count, B_1 and B_2 are standing background counts, T is the ratio of scan time to background time, $I = [CT - 0.5T(B_1 + B_2)]$, and P is a parameter used to avoid overweighting strong reflections and was set equal to 0.04.
(26) D. T. Cromer and J. T. Waber, *Acta Crystallogr.*, **18**, 104 (1965).
(27) R. F. Stewart, E. R. Davidson and W. T. Simpson, *J. Chem. Phys.*, **42**, 3175 (1965).
(28) D. T. Cromer and D. L. Liberman, *J. Chem. Phys.*, **53**, 1891 (1970).
(29) O. N. Krasochka, V. A. Avilov, and L. O. Atovmyan, *Zh. Strukt. Khim.*, **15**, 1140 (1974).
(30) M. Habenschuss and B. C. Gerstein, *J. Chem. Phys.*, **61**, 852 (1974).
(31) N. F. Curtis, I. R. N. McCormick, and T. N. Waters, *J. Chem. Soc., Dalton Trans.*, 1537 (1973).
(32) C. G. Pierpont, D. N. Hendrickson, D. M. Duggan, F. Wagner, and E. K. Barefield, *Inorg. Chem.*, **14**, 604 (1975).
(33) D. M. Duggan and D. N. Hendrickson, *Inorg. Chem.*, **13**, 2056 (1974).
(34) E. J. Laskowski, D. M. Duggan, and D. N. Hendrickson, *Inorg. Chem.*, **14**, 2449 (1975).
(35) D. M. Duggan and D. N. Hendrickson, *Inorg. Chem.*, **13**, 1911 (1974).
(36) E. J. Laskowski and D. N. Hendrickson, unpublished results.
(37) R. J. Sime, R. P. Dodge, A. Zalkin, and D. H. Templeton, *Inorg. Chem.*, **10**, 537 (1971).
(38) A. P. Ginsberg, R. L. Martin, R. W. Brookes, and R. C. Sherwood, *Inorg. Chem.*, **11**, 2884 (1972).
(39) R. West and D. L. Powell, *J. Am. Chem. Soc.*, **85**, 2577 (1963).
(40) B. Bleaney and K. D. Bowers, *Proc. R. Soc. London, Ser. A*, **214**, 451 (1952).
(41) A. P. Ginsberg and M. E. Lines, *Inorg. Chem.*, **11**, 2289 (1972).
(42) B. J. Hathaway and D. E. Billing, *Coord. Chem. Rev.*, **5**, 143 (1970).
(43) J. Owen and E. A. Harris in "Electron Paramagnetic Resonance", S. Geschwind, Ed., Plenum Press, New York, N.Y., 1972, Chapter 6.
(44) D. M. Duggan and D. N. Hendrickson, *Inorg. Chem.*, **13**, 2929 (1974).
(45) P. J. Hay, J. C. Thibeault, and R. Hoffmann, *J. Am. Chem. Soc.*, **97**, 4884 (1975).